Received: 16 January 2020 | Revised: 6 April 2020 | Accepted: 26 April 2020

DOI: 10.1111/jfs.12814

ORIGINAL ARTICLE

Journal of Food Safety WILEY

Gelatin nanocomposite films incorporated with magnetic iron oxide nanoparticles for shelf life extension of grapes

Zaffar Mehmood | Muhammad Bilal Sadiq | Muhammad Rehan Khan

School of Life Sciences, Forman Christian College (A Chartered University), Lahore, Pakistan

Correspondence
Muhammad Bilal Sadiq and Muhammad Rehan Khan, School of Life Sciences, Forman Christian College (A Chartered University), Lahore 54600, Pakistan.
Email: m.bilalsadiq@hotmail.com (M. B. S.) and rehankhan@fccollege.edu.pk (M. R. K.)

Funding information
Higher Education Commission, Pakistan, Grant/Award Number: 10413 NRPU

Abstract

Nanocomposite films were obtained by solution casting method from aqueous solution of bovine gelatin with addition of various concentrations of magnetic iron oxide (MIO) nanoparticles (NPs) (5, 10, 15, and 20% w/w of dry gelatin). The incorporation of MIO NPs improved the mechanical and physical properties of the nanocomposites. The increase in concentration of NPs up to 10% improved barrier and mechanical properties which slightly decreased after increasing the concentration beyond that limit due to particle agglomeration. The scanning electron microscopy and X-ray diffraction (XRD) were used to evaluate the morphology and crystalline structure of gelatin nanocomposite films, respectively. Gelatin nanocomposites with 20% w/w NPs exhibited the highest antimicrobial activity against *Escherichia coli* (7.1 ± 0.085 mm) and *Staphylococcus aureus* (8.22 ± 1.04 mm). Finally, the potential of gelatin/MIO nanocomposites as packaging material was evaluated to extend the shelf life of grapes. The gelatin/MIO nanocomposites can be used as a replacement to non-biodegradable packaging.

1 | INTRODUCTION

Food preservation plays an essential role in controlling physicochemical changes in variety of food products that is, fresh meat, vegetables, and fruits. It prolongs the shelf life of perishable food items by preventing them from oxidation reduction reactions and microbial spoilage (Hanani, Roos, & Kerry, 2014; Samsi, Kamari, Din, & Lazar, 2019). The traditional techniques such as salting, drying, smoking, and freezing are used to preserve food products. However, many of these traditional preservations techniques are associated with limitations, such as changes in organoleptic characteristics, hence unsuitable for food industries (Samsi et al., 2019). Petrochemical-based plastics are widely used in food industry due to their attractive qualities, that is, good tear and tensile strength (TS), abundant availability, and low cost (Basu et al., 2017; Hanani et al., 2014). However, due to non-biodegradable nature, synthetic petroleum-based packaging materials pose a public health and environmental concerns (Hanani et al., 2014). Recently, biopolymer-based biodegradable packaging materials have gained tremendous attention as an alternative to petrochemical-based packaging plastics and hence promote the reduction of environmental pollution by the use of green chemistry and can play an important role in achieving sustainable development goals proposed by UN especially achieving zero hunger by ensuring food security (Barra & Gonzalez, 2018; Chein, Sadiq, & Anal, 2019; Shankar, Wang, & Rhim, 2019). Due to biodegradable nature, gelatin-based food packaging films have been vastly studied to protect food from light, oxygen, and drying because of its good film forming ability, as an encapsulating material and as a carrier for bioactive compounds (Shankar et al., 2019). However, poor barrier and mechanical properties of gelatin-based films restrict their application as packaging material in food industry.

It is worth mentioning the phenomenon of miscibility of homopolymer-copolymer system by heat of mixing as it is attributed to the dilution of strong repulsive interaction between the monomer residues in the homopolymer with the monomer residues in the copolymer, with which repulsive interaction of the later is not as strong. An exothermic mixing usually outweighs the unfavorable equation of state influence on the thermodynamics of mixing. Miscible blends are therefore, encountered when specific interactions exist between the components (Rana, Mandal, & Bhattacharyya, 1993, 1996). Thus, barrier, mechanical, and thermodynamic properties of gelatin films can be improved by reinforcing gelatin structure with nano-sized fillers (Shankar et al., 2019; Shankar, Teng, Li, & Rhim, 2015). Generally, addition of nanoparticles (NPs) into polymer matrix can enhance the thermal properties of gelatin

nanocomposites by increasing the crystallinity of gelatin and can instigate compressive and ordered crystals (Sahraee, Ghanbarzadeh, Milani, & Hamishehkar, 2017). A variety of NPs such as nanoclays, metals, metal oxides and other nanofillers have been incorporated into gelatin film formulation (Shankar, Jaiswal, & Rhim, 2016). NPs have been reported to reinforce the gelatin matrix after entrapment; providing a twisted pass-way for the transport of water and oxygen vapors thus delaying their transport across the film (Sahraee et al., 2017; Shankar et al., 2019). The mechanical and barrier properties of gelatin composite films have been improved by the incorporation of NPs such as silver (Kumar, Mitra, & Halder, 2017), TiO_2 (Nassiri, 2018), zinc oxide (Marvizadeh, Oladzadabbasabadi, Nafchi, & Jokar, 2017), chitosan (Hosseini, Rezaei, Zandi, & Farahmandghavi, 2015), and montmorillonite (MMT) (Flaker, Lourenço, Bittante, & Sobral, 2015). Iron oxide (IO) NPs have been widely used in biomedical applications because of their magnetic properties and biocompatibility (Tran et al., 2010). IO NPs have been reported to inhibit the growth of different foodborne pathogens that is, *Escherichia coli*, *Pseudomonas aeruginosa*, and *Staphylococcus aureus* (Azam et al., 2012; Tran et al., 2010). IO NPs might be responsible for generating oxygen reactive species which can kill bacteria by damaging proteins and DNA; without harming the non-bacterial cells and can even enhance the proliferation of osteoblasts thus providing dual function (Tran et al., 2010). IO NPs are safe and non-cytotoxic up to 100 μg/ml concentration (Singh, Jenkins, Asadi, & Doak, 2010) and have also been reported as potential oral therapeutic agent for the treatment of iron deficiency anemia (Faria, Pereira, Mergler, & Powell, 2011).

In this study, magnetic iron oxide (MIO) NPs were used for the development of gelatin/MIO nanocomposite films. The influence of NP concentration on the mechanical, barrier, optical, antioxidant, and antibacterial properties of gelatin nanocomposites was investigated. Finally, the gelatin nanocomposite films were evaluated for their potential to extend the shelf life of grapes.

2 | MATERIALS AND METHODS

2.1 | Materials

MIO NPs with a mean particle size of (6.5 ± 3.0 nm), type B gelatin (bovine), DPPH (2, 2-Diphenyl-1-picrylhydrazyl), ABTS [2, 2′-Azino-bis (3-ethylbenzothiazoline-6-sulphonic acid)], and AAPH [2, 2′-Azobis (2-amidinnopropane) dihydrochloride] were purchased from Sigma Aldrich, (St. Louis, MO). All other chemicals used were of analytical grade.

2.2 | Preparation of gelatin nanocomposite films

The nanocomposite films of gelatin/MIO NPs were prepared by using a solution casting method given by Dammak, de Carvalho, Trindade, Lourenço, & do Amaral Sobral, 2017, with modifications. Film forming solutions (FFSs) was prepared by dissolving gelatin (4 g) into distilled water (80 ml) at room temperature, and then the mixture was stirred at 45°C and 150 rpm for 30 min in shaking incubator (Wisecube, Seoul, Korea). After cooling to 37°C, glycerol (0.25 g/g of dry gelatin) was added into the FFS and again the mixture was stirred for 30 min at 45°C and 150 rpm in shaking incubator. Finally, different concentrations (5, 10, 15, and 20% w/w of dry gelatin) of MIO NPs were added into gelatin FFS. Finally distilled water was added to complete the final volume of 100 ml. FFS was then homogenized at 6000 rpm for 5 min by using a homogenizer (Ultra-Turrax IKA T50, Wasserburg, Germany) followed by sonication (Heidolph, Schwabach, Germany) for 15 min to remove air bubbles.

FFS (25 ml) was cast into polystyrene petri plates (8 × 8 cm^2, St. Louis, MO) and allowed to dry in the oven (Memmert, ULM 500, Germany) for 15 hr at 45°C. The films were then peeled off carefully and placed in a desiccator before characterization.

2.3 | Film characterizations

2.3.1 | Thickness

Thickness of the film samples was measured by using a micrometer (model ID-C112PM, Mitutoyo, Japan).

2.3.2 | Mechanical properties

TS, elastic modulus (EM), and elongation at break (EAB) of the film samples were determined according to the standard ASTM (American Society for Testing and Materials) method D882-09 by using a universal testing machine (Model 5565, Instron Engineering Corporation, Canton, MA) in tensile mode. Initial grip separation and mechanical cross head speed were set at 40 mm and 5 mm/min, respectively, with a load cell of 500 N.

2.3.3 | Film water solubility

Water solubility (WS) of the film samples was determined by following the method as described by Nur Hanani, Beatty, Roos, Morris, and Kerry (2013) with slight modifications. Briefly, film samples were cut into 4 × 4 cm^2 strips and weighed then dried in oven for 24 hr at 105°C. Each dried sample was then dipped into 100 ml distilled water for 24 hr. After removing from the solution, the film samples were again redried for 24 hr at 105°C. Final weight of the samples was noted and film WS was calculated by following Equation 1.

$$WS\% = \frac{\text{Initial weight} - \text{Final weight}}{\text{Initial weight}} \times 100. \quad (1)$$

2.3.4 | Water vapor permeability

Water vapor permeability (WVP) of the film samples was determined, gravimetrically, according to a standard method given by ASTM E96-

95 with slight modifications (Kanmani & Rhim, 2014). WVP of the gelatin nanocomposite films was determined by using special Fisher cups with an average width and depth of 6.8 and 2.5 cm, respectively. Each film sample was cut into rectangular pieces of 7×7 cm^2 and then placed onto the top of the cups containing 18 ml of distilled water. A topper was used to cover the cups and tightened by using screws. The cups were placed inside a humidity chamber set at 25°C and 50% relative humidity (RH). The weight loss of each cup was measured for 8 hr at 1 hr intervals. The WVP (g m/m^2 s Pa) was calculated by using Equation (2).

$$WVP = \frac{WVTR \times L}{\Delta p} \quad (2)$$

where WVTR = water vapor transmission rate (g/m^2 s) was measured, L = thickness of the film (m), and Δp = partial water vapor pressure difference (Pa) across the film samples.

2.3.5 | Oxygen permeability

Oxygen permeability (OP) of gelatin nanocomposite films was measured according to ASTM D3985 method (Abdellatief & Welt, 2013), through an Ox-Tran 2/21 modular system (Mocon, Inc., Minneapolis, MN). The film samples (2×2 cm^2) were placed on a stainless steel mask with 5 cm^2 testing area. The mask was then exposed to 98% N_2+ 2% H_2 flow from one side and 100% O_2 from the other side after placing in a test cell. Film samples were allowed to stabilize for 10 hr before readings were taken. Oxygen transmission rates were measured at 55% RH and 25°C. OP was obtained by dividing oxygen transmission rate by oxygen partial pressure difference and multiplying with average film thickness.

2.3.6 | Apparent surface color and transparency of film samples

The color of the film samples was measured by using a chroma meter (Minolta, CR 10, Tokyo, Japan). The total color difference (ΔE) was measured by using a white standard color plate with hunter color values (L^* = 92.7; a = 1.51*; b^* = −5.9) as a background to measure surface color of the film samples. For each film sample a total of six replicates were measured to get average hunter color (CIE L^*, a^*, and b^*) values. ΔE was calculated by following Equation (3).

$$\Delta E^* = \left[(\Delta L^*)^2 + (\Delta a^*)^2 + (\Delta b^*)^2\right]^{0.5} \quad (3)$$

whereas ΔL^*, Δa^*, and Δb^* are the differences between the color of standard color plate and film samples (Kanmani & Rhim, 2014).

Transparency of film samples was expressed as percent transmittance measured at 660 and 280 nm at visible and UV region, respectively. For this, a rectangular piece of film sample was cut and clamped directly between the magnetic cell holders of UV–vis spectrophotometer (Cecil series 2021, Cecil Instruments Limited, UK). Three replicates were measured and average values were presented (Kanmani & Rhim, 2014).

2.4 | Antioxidant activities of the films

2.4.1 | DPPH radical scavenging assay

The DPPH radical scavenging activity of gelatin nanocomposites was determined by a method given by Sadiq, Hanpithakpong, Tarning, and Anal (2015) with slight modifications. For this, 100 μL of FFS was added into freshly prepared 5 ml of 40 ppm methanol solution of DPPH. The mixture was incubated in dark with shaking for 45 min at 25°C. After incubation the absorbance was read at 517 nm against blank. L-ascorbic acid was used as a positive control. DPPH inhibition (%) was calculated by using Equation (4)

$$DPPH\%inhibition = \frac{(AC - AS)}{AC} \times 100 \quad (4)$$

where AC is the absorbance of control and AS is the absorbance of sample.

2.4.2 | $ABTS^+$ radical scavenging assay

$ABTS^+$ radical scavenging was measured by following the method of Shankar et al. (2019) with slight modifications. Briefly, $ABTS^+$ radical solution was prepared by mixing 100 ml of 1 mM AAPH solution and 100 ml of 2.5 mM of $ABTS^+$ solution and resultant solution was incubated for 45 min at 60°C in the dark. The pH of the $ABTS^+$ solution was adjusted to 7.4 with phosphate buffer saline. For the assay, 300 μL of FFS was taken and dissolved in 2700 μL of $ABTS^+$ solution and incubated for 30 min in the dark place. The absorbance was read at 734 nm by UV–vis spectrophotometer. Percentage inhibition was calculated by using Equation (5).

$$ABTS^+\%inhibition = \frac{(AC - AS)}{AC} \times 100 \quad (5)$$

where AC is the absorbance of $ABTS^+$ solution (control) and AS is the absorbance of $ABTS^+$ solution and FFS (sample).

2.5 | Antibacterial activity

Antibacterial activity of gelatin/MIO nanocomposite films was determined by agar diffusion assay as described by Iamareerat, Singh, Sadiq, and Anal (2018) with slight modifications. The gelatin nanocomposite films were cut into 4 mm disks (sterilized by UV light for 1 hr) and placed on the surface of Mueller-Hinton agar

plates inoculated with *E. coli* ATCC 8739 and *S. aureus* ATCC 25923. The plates were then incubated for 24 hr at 37°C and antibacterial activity was measured by measuring the inhibition zones around the films.

2.6 | Film structure

2.6.1 | Fourier-transform infrared spectroscopy

Chemical structure of gelatin nanocomposites was analyzed by using Fourier-transform infrared spectroscopy (FT-IR) spectrometer (Model: Cary 630, Agilent Technologies, Santa Clara, CA) coupled with a universal attenuator total reflectance accessory. Spectra were recorded in the range of 4,000–650 cm^{-1} with 4 cm^{-1} resolution.

2.6.2 | X-ray diffraction

The X-ray diffraction (XRD) was used, in order to study the phase distribution and crystalline structure of gelatin nanocomposites. Films were cut into square pieces (2×2 cm^2) and held on a X-ray diffractogram (Siemens, model D5000), and diffractograms were measured at 40 kV and 40 mA with 1.540 Å using Cu Kα. The diffraction angles of 2θ = 10–85° were set to determine relative intensity at room temperature (Sahraee et al., 2017).

2.6.3 | Microstructure of gelatin nanocomposites

To study the surface morphology of gelatin nanocomposites, scanning electron microscopy (SEM) (ZEISS EVO, Thornwood, NY) was applied according to the method given by Sahraee et al. (2017) with slight modifications. Small pieces of film samples were held on the SEM specimen stage, and an acceleration voltage of 20 kV was used. Before SEM analysis, the samples were coated with gold using a vacuum sputter coater.

2.7 | Preservation studies

2.7.1 | Weight loss and browning index

The gelatin nanocomposite films were used to extend the shelf life of grapes. The fresh of approximately the same shape, size, color, and maturity were wrapped with each nanocomposite film sample. For control treatments, grapes were wrapped with plastic (polyethylene) film and neat gelatin film, and also grapes were stored unwrapped under the same conditions. The samples in triplicates were kept at 25°C to simulate the conditions, in which they are kept by local retailers and vendors, and the packaged fruits were observed for weight loss and browning index daily. The percentage of fruit weight loss was calculated by Equation (6).

$$\text{Weight loss}\,(\%) = \frac{(Wi - Wf)}{Wi} \times 100 \quad (6)$$

where W_i is the initial weight of the fruit and W_f is the final weight of the fruit after 14 days of preservation study. The browning index was calculated by using Equation (7) (Samsi et al., 2019).

$$\text{Browning index} = \frac{\Sigma\,(\text{Browning level}) \times \text{number of fruits at browning level}}{\text{Total number of fruits in the treatment}} \times 100. \quad (7)$$

Priya, Suriyaprabha, Yuvakkumar, and Rajendran (2014) classified the browning level as: 1 = no browning, 2 = less than 20%, 3 = around 20–40%, 4 = around 40–60%, and 5 => 60%.

2.7.2 | Microbiological analysis

Microbiological analysis of grapes was done according to the method given by Tornuk, Hancer, Sagdic, and Yetim (2015) with modifications. The grapes of approximately similar shape, size, and color were washed with distilled water twice and were disinfected by UV light for 10 min. After preparing the inoculum, the grapes were dipped into microbial suspension of *S. aureus* (10^4 CFU/ml) for 90 s. After draining, the fruit samples were kept at room temperature for 1 hr in order to facilitate surface drying and bacterial adhesion. Finally, inoculated fruit samples were wrapped in gelatin nanocomposites of 6×6 cm^2 squares. Control samples were kept unwrapped and packed in simple gelatin and plastic (polyethylene) films. Wrapped samples were stored at 25°C for 5 days and microbial analysis was done daily by calculating CFU/g of the packed samples. Briefly, fruit samples at each interval of time were homogenized in 0.1% of peptone saline solution for 10 s in a sterile stomacher (Stomacher 400, Lab, Blender, London, UK). After incubation total colonies were counted and expressed as CFU/g of the fruit sample (Khan, Sadiq, & Mehmood, 2020).

2.8 | Statistical analysis

One-way analysis of variance was performed to estimate the significant differences ($p < .05$) between mean observations by using SPSS statistical software package (SPSS, version 23.0, Inc., Chicago, IL).

3 | RESULTS AND DISCUSSION

3.1 | Film characterization

3.1.1 | Thickness

The thickness of the gelatin nanocomposite films increased with increasing concentration of MIO NPs (Table 1). The thickness of the

TABLE 1 Physicochemical characterization of neat gelatin and gelatin/magnetic iron oxide nanoparticle (MIO NP)-based nanocomposite films

Samples	Thickness (mm)	Tensile strength (MPa)	Elongation at break (%)	Elastic modulus (MPa)	Water solubility (%)	Water vapor permeability ($\times 10^{-9}$ g/m^2 Pa s)	Oxygen permeability (cm^3 µm/m^2 day kPa)	ΔE	T_{280} (%)	T_{660} (%)
Gelatin	0.17 ± 0.0005^{d}	8.78 ± 0.60^{c}	38.98 ± 1.02^{a}	257.41 ± 3.48^{d}	79.34 ± 1.06^{a}	3.94 ± 0.03^{a}	4.28 ± 0.04^{a}	4.06 ± 0.35^{e}	67.72 ± 0.30^{a}	85.69 ± 0.15^{a}
Gelatin + MIO NPs 5%	0.172 ± 0.0005^{c}	11.44 ± 0.39^{b}	32.84 ± 0.46^{b}	299.30 ± 2.61^{c}	76.99 ± 0.26^{b}	3.78 ± 0.03^{b}	4.11 ± 0.08^{ab}	7.26 ± 0.37^{d}	66.57 ± 0.35^{b}	83.83 ± 0.23^{b}
Gelatin + MIO NPs 10%	0.173 ± 0.001^{c}	12.56 ± 0.09^{a}	27.92 ± 0.24^{c}	332.81 ± 3.24^{a}	72.97 ± 2.5^{c}	3.36 ± 0.04^{c}	3.93 ± 0.06^{b}	8.13 ± 0.20^{c}	65.7 ± 0.33^{c}	83.12 ± 0.02^{c}
Gelatin + MIO NPs 15%	0.178 ± 0.0005^{b}	11.25 ± 0.35^{b}	25.9 ± 0.22^{d}	323.93 ± 4.43^{ab}	73.32 ± 0.11^{c}	3.40 ± 0.038^{c}	3.96 ± 0.03^{b}	9.28 ± 0.21^{b}	65.06 ± 0.07^{c}	82.65 ± 0^{c}
Gelatin + MIO NPs 20%	0.183 ± 0.001^{a}	11.09 ± 0.10^{b}	25.84 ± 0.05^{d}	321.56 ± 4.33^{b}	73.59 ± 0.55^{c}	3.42 ± 0.026^{c}	3.97 ± 0.15^{b}	10.23 ± 0.15^{a}	63.23 ± 0.35^{d}	81.64 ± 0.27^{d}

Note: Different superscript letters (a–d) within a column indicate significant ($p < .05$) differences among mean observations.

control (without NPs) gelatin film was 0.17 mm, which increased to 0.183 mm after incorporation of 20% NPs. The increase in thickness of the gelatin nanocomposites films might be due to increase in solid content of the FFS. Jorge et al. (2015) also reported an increase in thickness of gelatin nanocomposites (from 0.071 to 0.080 mm) with increasing concentration of MMT NPs (5 to 10 g/100 g of gelatin) due to increase in the solid content of FFS.

3.1.2 | Mechanical properties

The mechanical properties (TS and EM) of gelatin nanocomposite films increased linearly with increasing concentration of NPs from 5 to 10% followed by a decrease, with further increase in NPs (Table 1). This might be due to the fact that the NPs reinforced the gelatin matrix thus producing a strong network up to a critical concentration further increase in the concentration of NPs led to jamming of NPs into the matrix (Arfat, Ahmed, Hiremath, Auras, & Joseph, 2017). The matrix of gelatin could not hold additional NPs and the distribution of MIO NPs in the protein matrix was not uniform, thus, the TS and EM for gelatin nanocomposite film containing 15 and 20% NPs were decreased. On the other hand, EAB of the gelatin nanocomposites decreased (from 38.98 to 25.84%) linearly with increasing concentration of NPs from 5 to 20% due to improved rigidity of the nanocomposite films. MIO NPs have been reported to agglomerate at high concentration due to their hydrophobic nature, thus reducing the mechanical properties of films by impeding the amorphous network of the gelatin nanocomposites and protein domain arrangements (Arfat et al., 2017; Zhu et al., 2018).

3.1.3 | Water solubility of films

Film WS is an important characteristic of biodegradable films as they are used to package the food. Certain applications of packaging films may require water insolubility to enhance water resistance and product integrity (Hosseini et al., 2015). The WS of control gelatin films was 79.34%, whereas the addition of MIO NPs up to 10% into gelatin film matrix resulted a decrease in WS (from 79.34 to 72.97%) of gelatin nanocomposites. However, with further increase in concentration of NPs (10 to 20%) there was no significant change in WS of gelatin composite films. The control gelatin films exhibited high WS due to hydrophilic nature of the gelatin, whereas the addition of NPs resulted in the formation of hydrogen bonds between NPs and gelatin matrix which in turn decreased the WS (Voon, Bhat, Easa, Liong, & Karim, 2012).

3.1.4 | Water vapor permeability

High WVP of the food packaging films is a problem for food industries. WVP of the gelatin film was decreased from 3.94 ± 0.03 to 3.36 ± 0.04 ($\times 10^{-9}$ g/m^2 Pa s) after reinforcing the gelatin matrix with NPs from 0 to 10%. However, WVP of gelatin composites films was

not significantly different as the concentration of NPs was increased from 10 to 20% in gelatin matrix (Table 1).

The addition of NPs in biopolymer matrix can reduce the water permeability by developing three dimensional tightly linked networks (De Moura et al., 2009). Hosseini et al. (2015) reported that addition of chitosan NPs resulted in twisted pathways across the gelatin film matrix thus hinder the passage of water molecules through the matrix. The decrease in WVP of gelatin composite films might be attributed to restricted movement of protein molecules after incorporation of NPs into gelatin matrix (Vanin et al., 2014). However, additional incorporation of MIO NPs (i.e., 15 and 20%) led to aggregation, which reduced the effective content of NPs thus, facilitated permeation of water vapors. Generally, NPs can reduce the WVP by reducing the free hydroxyl groups (NH, OH) and/or by increasing the crystallinity of gelatin matrix thus creating a torturous pathway for the diffusion of water molecules across the film matrix (Shankar et al., 2019).

3.1.5 | Oxygen permeability

The high OP may lead to oxidative deterioration of the packed food products (Samsi et al., 2019). Therefore, controlling the permeation of oxygen molecules is essential to ensure the quality and freshness of fresh produce. OP of neat gelatin film was decreased significantly (from 4.28 to 3.93 $cm^3 \mu m/m^2$ day kPa) after incorporation of 10% NPs into gelatin matrix; however, further increase in concentration (10 to 20%) of NPs did not cause any significant change in OP of gelatin composite films. Nafchi, Nassiri, Sheibani, Ariffin, and Karim (2013) reported a decrease in OP of the sago starch and gelatin-based nanocomposite films with increasing concentration of zinc oxide nanorod from 1 to 5% (w/w), which was attributed to adhesion of NPs with biopolymer matrix thus decreasing the oxygen transport by reducing free volume.

3.1.6 | Total color difference and transparency

Product demand and consumer preferences might be influenced by the color of the packaging film. The neat gelatin films exhibited significantly lower ΔE values (4.06 ± 0.35) as compared to gelatin/MIO NP nanocomposites. The neat gelatin films were almost transparent (characteristic of gelatin films). On the other hand, for gelatin nanocomposite films; ΔE values were increased with increasing concentration of NPs from 5 to 20% (w/w) (from 7.26 to 10.23). An increase in the value of ΔE indicates successful incorporation of MIO NPs within gelatin matrix. Kanmani and Rhim (2014) reported that ΔE was increased (from 2.1 to 61.4) with increasing concentration (from 10 to 40 mg) of silver NPs in the film matrix due to incorporation of silver NPs into the film matrix.

Transparency of the packaging materials prevents light transmission and provides the ability to see through the packaging materials and is one the most important physical parameters of films. The incorporation of MIO NPs into gelatin matrix reduced the transmittance of gelatin nanocomposites for visible and UV regions. The neat gelatin films were very transparent with transmittance of 85.69 and 67.72% for visible (660 nm) and UV (280 nm) regions, respectively (Table 1). Percentage transmittance decreased with increasing concentration of NPs into the FFS. It has been reported that percentage transmittance of gelatin/ silver nanocomposites in visible region decreased significantly (from 85.6 to 49.6%) with increasing concentration of silver NPs (from 10 to 40 mg) (Kanmani & Rhim, 2014).

3.2 | Antioxidant activity

The neat gelatin films showed significantly lower radical scavenging activity value of 6.32 ± 0.21 and 7.93 ± 0.14% for DPPH and $ABTS^+$ assay, respectively. On the other hand, after the incorporation of MIO NPs into gelatin FFS, the antioxidant activities of gelatin nanocomposites were significantly increased with increase in concentration of NPs. Maximum radical scavenging activity was observed for gelatin nanocomposites containing 20% NPs (w/w) with values of 55.07 and 56.98% for DPPH and $ABTS^+$, respectively (Table 2). It has been reported that antioxidant activity of packaging films is directly proportional to amount of antioxidant added (Shankar et al., 2019). These results corroborate with the previous study which reported an increase in %DPPH inhibition with increasing concentration of IO particles (Paul, Saikia, Samdarshi, & Konwar, 2009).

3.3 | Antibacterial activity

The neat gelatin films showed no inhibition against the test pathogens, whereas after the incorporation of MIO NPs into gelatin FFS, the inhibition zones were observed against *E. coli* and *S. aureus*. The gelatin nanocomposite films containing 20% MIO NPs showed significantly higher inhibition against *S. aureus* (8.22 ± 1.04 mm) and *E. coli* (7.10 ± 0.08 mm) (Table 2). It has been previously reported that metal oxide NPs are more effective against gram-positive bacteria than gram-negative (Azam et al., 2012). The zero valent iron NPs can cause physical disruption of the cell membrane of bacteria; while reaction of Fe (II) with intracellular hydrogen peroxide or oxygen can also lead to the production of reactive oxygen species thus inducing oxidative stress in bacteria (Lee et al., 2008).

3.4 | Film structure

3.4.1 | Fourier-transform infrared spectroscopy

FT-IR was carried out to study the chemical interactions between the gelatin film matrix and NPs. Distinct amide bands in the gelatin are generally associated with the triple helix structure (Sahraee et al., 2017). Thus, peaks around 3,200–3,500 cm^{-1} are associated with amide A and amide B, which include O-H and N-H stretching vibration; and the wide peak in this region may indicate overlapping of type II amide N-H stretching peaks and amines (Liu, Antoniou, Li, Ma, & Zhong, 2015). Another significant peak around 2,942 cm^{-1} is related to asymmetric and symmetric C-H stretching frequency

TABLE 2 Antioxidant and antibacterial activities of gelatin nanocomposite films

Samples	Antioxidant activities		Antibacterial activities (ZI in mm)	
	DPPH (%)	$ABTS^+$ (%)	*S. aureus*	*E. coli*
Gelatin	6.32 ± 0.21^{e}	7.93 ± 0.14^{e}	0	0
Gelatin + MIO NPs 5%	20.24 ± 0.45^{d}	23.72 ± 0.98^{d}	5.33 ± 0.15^{c}	4.7 ± 0.2^{d}
Gelatin + MIO NPs 10%	30.87 ± 0.69^{c}	31.18 ± 0.44^{c}	6.3 ± 0.31^{bc}	5.68 ± 0.20^{c}
Gelatin + MIO NPs 15%	42.19 ± 0.65^{b}	44.22 ± 1.16^{b}	7.53 ± 0.13^{ab}	6.32 ± 0.22^{b}
Gelatin + MIO NPs 20%	55.07 ± 1.16^{a}	56.98 ± 3.14^{a}	8.22 ± 1.04^{a}	7.10 ± 0.08^{a}

Note: Different superscript letters (a–e) within a column indicate significant ($p < .05$) differences among mean observations.
Abbreviations: MIO NP, magnetic iron oxide nanoparticles; ZI, zone of inhibition.

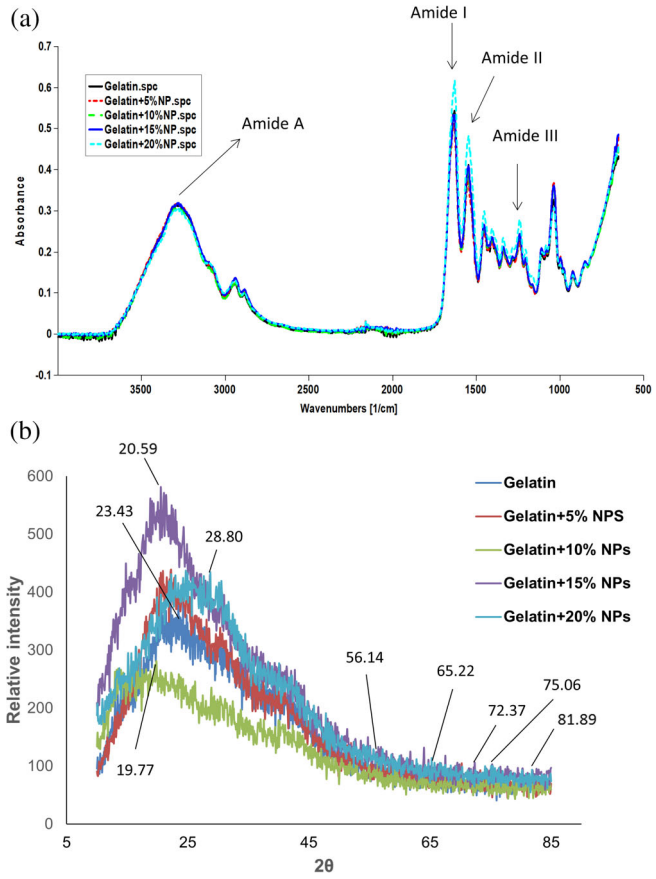

FIGURE 1 (a) Fourier transform infrared spectra of neat gelatin and gelatin nanocomposites. (b) X-ray diffraction (XRD) patterns of neat gelatin and gelatin nanocomposites

(Sahraee et al., 2017). Two significant peaks around 1,630 and 1,548 cm^{-1} are corresponding to stretching vibrations of N-H and C=O groups involved in peptide band of amide I and amide II structures, respectively. The characteristic band for amide III region was observed at 1240 cm^{-1} representing N-H bending and C-N stretching vibrations (Figure 1a). Additionally, this peak can also be linked with proline and glycine backbone of the chains (Liu et al., 2015). Glycerol presence in film formulation was confirmed by the peak at 1037 cm^{-1}; similarly, Sahraee et al. (2017) reported amide I, II, and III peaks around 1,652, 1,558, and 1,220 cm^{-1}, respectively, for neat gelatin films.

On the other hand, FT-IR spectra of gelatin nanocomposites containing MIO NPs were relatively similar to neat gelatin films. However, slight shift in some peaks was observed with increasing concentration of NPs in gelatin matrix. N-H stretching band was transferred from 3,283 to 3,291 cm^{-1} after incorporation of 10% NPs in gelatin matrix indicating a possible formation of hydrogen bonding between NPs and polymer matrix; with increasing concentration of NPs above 10% the spectra shifted to as low as 3,278 cm^{-1} for gelatin films containing 15% NPs due to agglomeration of NPs. Furthermore, amide I peak for gelatin nanocomposite containing 15% NPs was observed at 1638 cm^{-1}. Hosseini et al. (2015) similarly reported shifting of amide A and amide II bands to a higher wave number due to hydrogen bonding between chitosan NPs and gelatin matrix. The shift of amide II band to a higher wave number was also attributed to hydrogen bonding between nanoclay and polymer matrix (Kanmani & Rhim, 2014). A shift of stretching vibrations of thiocyanate group (S-C ≡ N) to a higher wave number for gelatin nanocomposites was observed (2159–2,162 cm^{-1}) as compared to neat gelatin film (2,152 cm^{-1}) which could be responsible for antimicrobial potential of gelatin/MIO NPs nanocomposites; since allyl iso thiocyanates reported to possess antimicrobial activity against various foodborne pathogens (Lin, PRESTON III, & Wei, 2000).

3.4.2 | X-ray diffraction

The characteristic peak corresponding to amorphous phase was observed in film diffractogram at 2θ of 23.43° which associated with amorphous phase of neat gelatin and as well as gelatin composite films (Sahraee et al., 2017). After incorporation of NPs into gelatin films, additional peaks were observed in the diffractogram of gelatin (Figure 1b). These peaks were located at 2θ of at 28.80, 56.14, 65.22, 72.37, 75.06, and 81.89°, corresponded to (375.24), (107.85), (104.5), (106), (98.89), and (78.82) planes of MIO NPs (Maity & Agrawal, 2007) and can be used as an indication of crystalline nature of gelatin nanocomposites. This can also be correlated to the fact that lower concentration of NPs (i.e., 5 and 10% w/w) resulted in appropriate distribution and interaction of NPs with gelatin chains thus creating torturous pass-way for passage of water vapors. The overall crystallinity of the gelatin nanocomposites was increased after incorporation of MIO NPs (Rubentheren, Ward, Chee, & Tang, 2015). Additionally, some peaks

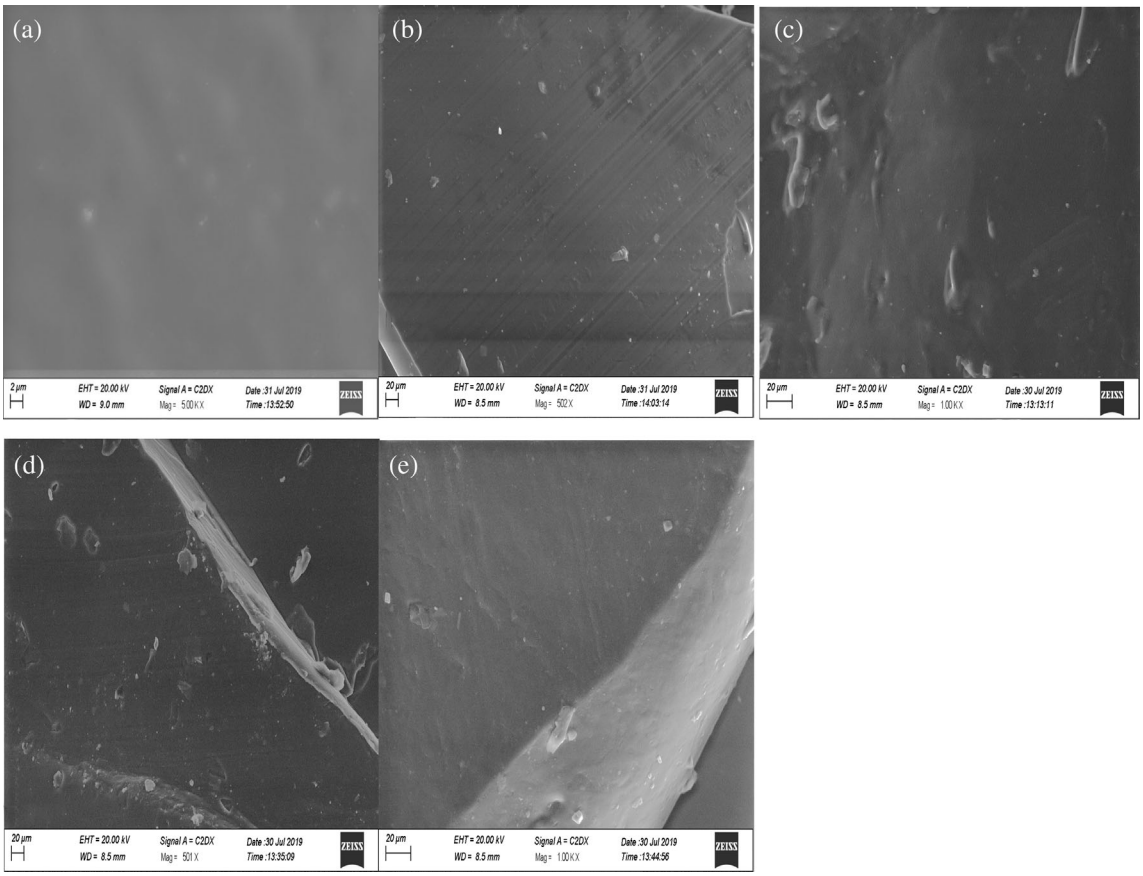

FIGURE 2 Scanning electron microscopy (SEM) micrographs of neat gelatin and gelatin nanocomposites. (a) Neat gelatin. (b) Gelatin + 5% w/w NPs. (c) Gelatin + 10% w/w NPs. (d) Gelatin + 15% w/w NPs. (e) Gelatin + 20% w/w NPs

TABLE 3 Percentage of weight loss and browning index of grapes at 25°C after 14 days of preservation

Samples	Weight loss (%)	Browning index
Gelatin	35.73 ± 1.86^{bc}	484.66 ± 13.05^{b}
Gelatin + MIO NPs 5%	34.62 ± 3.21^{bcd}	460.33 ± 15.69^{bc}
Gelatin + MIO NPs 10%	26.85 ± 1.50^{cde}	439.33 ± 9.50^{cd}
Gelatin + MIO NPs 15%	24.10 ± 3.91^{de}	430.66 ± 7.37^{cd}
Gelatin + MIO NPs 20%	21.5 ± 1.48^{e}	412.33 ± 10.59^{d}
Plastic bag	39.52 ± 4.11^{ab}	470.66 ± 5.03^{b}
Unwrapped	49.96 ± 7.18^{a}	519 ± 11.13^{a}

Note: Different superscript letters (a–e) within a column indicate significant ($p < .05$) differences among mean observations. MIO NP means magnetic iron oxide nanoparticle.

disappeared at higher concentrations (i.e., 20% w/w) of MIO NPs due to agglomeration of NPs which led to slightly reduced barrier and mechanical properties as compared to low NP concentrations.

3.4.3 | SEM

The surface morphology of gelatin nanocomposites was observed by SEM (Figure 2). Neat gelatin films displayed smooth and homogenous surfaces, with excellent structural integrity and without pores but gelatin nanocomposites containing NPs had rough surfaces along with cracks (Hosseini, Rezaei, Zandi, & Farahmandghavi, 2016). At low NP concentration (i.e., 5 and 10% w/w), most of the NPs were uniformly dispersed in gelatin matrix without agglomeration thus, enhanced mechanical strength (Sahraee et al., 2017). A reduced OP and WVP were observed due to twisted pass-way created by uniform dispersion of NPs across film. Slight aggregation of NPs was observed in gelatin matrix when concentration of NPs was increased above 10%. It has been reported that increasing concentration of NPs in the film matrix led to aggregation matrix which could increase chain interfaces and reduce cross linking of NPs with polymer matrix (Sahraee et al., 2017).

3.5 | Preservation studies

3.5.1 | Weight loss and browning index

The effectiveness of gelatin nanocomposites was evaluated by % weight loss and browning index of grapes after 14 days of storage at 25°C. The decaying process of fruit samples was monitored as the browning spots were seen and the outer membrane of grapes started to shrink. The soft texture and shrinkage on outer membrane might

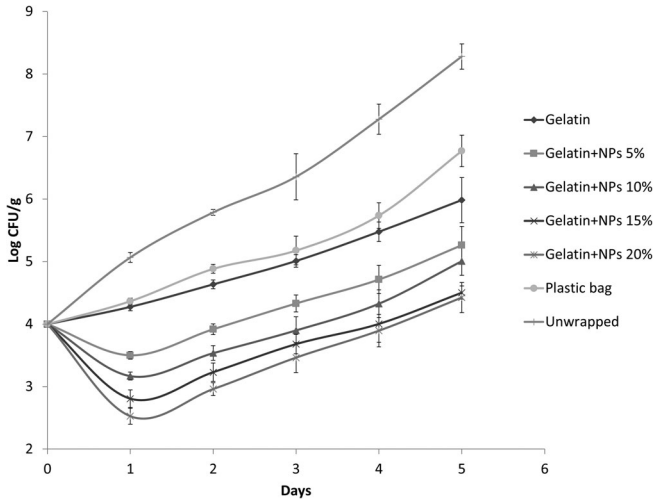

FIGURE 3 Shelf life of grapes packed in different packaging materials after artificial inoculation with *S. aureus*

be due to oxidation activities of polyphenols inside the fruits (Samsi et al., 2019). The grapes subjected to preservation treatments; unwrapped, gelatin and plastic packaging treatments showed high weight loss and browning index (Table 3). The fruit samples preserved in neat gelatin and plastic films presented strong decaying odor along with significant moldy spots after 8 days of storage. Fruit samples preserved in gelatin nanocomposite films containing 20% (w/w) NPs did not present any mildew and/or browning signs till the end of storage period and resulted in lowest values for weight loss and browning index, suggesting better preservation over other preservation treatments (Figure S1). Previously it was reported that addition of silver NPs into chitosan/gelatin FFS extended the shelf life of red grapes by 14 days (Kumar, Shukla, Baul, Mitra, & Halder, 2018).The ability of the films to preserve fruits was greatly influenced by the barrier properties, antibacterial and antioxidant potential, thus supporting the results of preservation studies.

3.5.2 | Microbiological analysis

The gelatin nanocomposites were further evaluated for their potential in preserving grape samples artificially inoculated with *S. aureus*. Gelatin nanocomposite films containing 20% (w/w) of MIO NPs not only inhibited the growth of *S. aureus* by reducing Log CFU/g below 2.6 but also kept the microbial limit below 4 log CFU/g (i.e., maximum allowable microbial limit for fruits recommended by FDA) until day 5, followed by 4 days for gelatin nanocomposites containing 15% NPs (w/w) (Figure 3). While the control treatments; grapes kept unwrapped and wrapped in neat gelatin and plastic films exceeded the microbial limit within 24 hr. Aitboulahsen et al. (2018) developed gelatin bioactive packaging incorporated with *Mentha pulegium* essential oil (1%) and observed the shelf life extension of strawberries even after 13 days of storage as compared to neat gelatin and control. Radi, Firouzi, Akhavan, and Amiri (2017) similarly studied the influence of gelatin-based packaging incorporated with *Aloe vera* and black and green tea extracts on the shelf life of freshly cut oranges and observed that microbial count of gelatin coatings incorporated with 10% green tea extract was lowest (4.17 log CFU/g) after 17 days of storage as compared to other treatments while fruit samples coated with only 1% gelatin exhibited higher microbial count as compared to other treatments after 17 days.

In this study, the concentration of MIO NPs used was lower than the reported safe range, therefore the residual analysis of NPs in the food sample was not evaluated. However, follow up studies should also consider the residual analysis of NPs in the food product during shelf life, their interactions with the food materials and safety evaluation.

4 | CONCLUSIONS

The incorporation of MIO NPs into gelatin films improved their barrier and mechanical properties indicating that the NPs enhanced the film applicability as biodegradable packaging. Furthermore, addition of IO NPs in gelatin films imparts the preservation potential in packaging films. Gelatin nanocomposites due to their hydrophobic, antibacterial, and antioxidant potential can serve as an alternative to plastic-based packaging for the preservation of fresh produce.

ACKNOWLEDGMENTS

This research was supported by Project (10413) titled "Development of Packaging Materials for Nanopreservation of Fresh Foods" by Higher Education Commission, Pakistan.

CONFLICT OF INTEREST

The authors declare no conflicts of interest.

AUTHOR CONTRIBUTIONS

Zaffar Mehmood and Muhammad Bilal Sadiq set the scope of this work and interpreted the experimental data. Muhammad Rehan Khan performed the experiments and drafted the manuscript.

ORCID

Zaffar Mehmood https://orcid.org/0000-0001-6557-7220
Muhammad Rehan Khan https://orcid.org/0000-0002-6110-583X

REFERENCES

Abdellatief, A., & Welt, B. A. (2013). Comparison of new dynamic accumulation method for measuring oxygen transmission rate of packaging against the steady-state method described by ASTM D3985. *Packaging Technology and Science*, *26*(5), 281–288.

Aitboulahsen, M., Zantar, S., Laglaoui, A., Chairi, H., Arakrak, A., & Bakkali, M. (2018). Gelatin-based edible coating combined with *Mentha pulegium* essential oil as bioactive packaging for strawberries. *Journal of Food Quality*, *2018*, 8408915. https://doi.org/10.1155/2018/8408915.

Arfat, Y. A., Ahmed, J., Hiremath, N., Auras, R., & Joseph, A. (2017). Thermo-mechanical, rheological, structural and antimicrobial properties of bionanocomposite films based on fish skin gelatin and silver-copper nanoparticles. *Food Hydrocolloids*, *62*, 191–202.

Azam, A., Ahmed, A. S., Oves, M., Khan, M. S., Habib, S. S., & Memic, A. (2012). Antimicrobial activity of metal oxide nanoparticles against gram-positive and gram-negative bacteria: A comparative study. *International Journal of Nanomedicine*, *7*, 6003.

Barra, R., & Gonzalez, P. (2018). Sustainable chemistry challenges from a developing country perspective: Education, plastic pollution, and beyond. *Current Opinion in Green and Sustainable Chemistry*, *9*, 40–44.

Basu, A., Kundu, S., Sana, S., Halder, A., Abdullah, M. F., Datta, S., & Mukherjee, A. (2017). Edible nano-bio-composite film cargo device for food packaging applications. *Food Packaging and Shelf Life*, *11*, 98–105.

Chein, S. H., Sadiq, M. B., & Anal, A. K. (2019). Antifungal effects of chitosan films incorporated with essential oils and control of fungal contamination in peanut kernels. *Journal of Food Processing and Preservation.*, *43*(12), e14235.

Dammak, I., de Carvalho, R. A., Trindade, C. S. F., Lourenço, R. V., & do Amaral Sobral, P. J. (2017). Properties of active gelatin films incorporated with rutin-loaded nanoemulsions. *International Journal of Biological Macromolecules*, *98*, 39–49.

De Moura, M. R., Aouada, F. A., Avena-Bustillos, R. J., McHugh, T. H., Krochta, J. M., & Mattoso, L. H. (2009). Improved barrier and mechanical properties of novel hydroxypropyl methylcellulose edible films with chitosan/tripolyphosphate nanoparticles. *Journal of Food Engineering*, *92*(4), 448–453.

Faria, N., Pereira, D., Mergler, B., & Powell, J. (2011). *Ligand doping of iron oxide nanoparticles as an approach to novel oral iron therapeutics*. The 2011 11th IEEE International Conference on Nanotechnology, IEEE. pp. 837–840.

Flaker, C. H., Lourenço, R. V., Bittante, A. M., & Sobral, P. J. (2015). Gelatin-based nanocomposite films: A study on montmorillonite dispersion methods and concentration. *Journal of Food Engineering*, *167*, 65–70.

Hanani, Z. N., Roos, Y. H., & Kerry, J. P. (2014). Use and application of gelatin as potential biodegradable packaging materials for food products. *International Journal of Biological Macromolecules*, *71*, 94–102.

Hosseini, S. F., Rezaei, M., Zandi, M., & Farahmandghavi, F. (2015). Fabrication of bio-nanocomposite films based on fish gelatin reinforced with chitosan nanoparticles. *Food Hydrocolloids*, *44*, 172–182.

Hosseini, S. F., Rezaei, M., Zandi, M., & Farahmandghavi, F. (2016). Development of bioactive fish gelatin/chitosan nanoparticles composite films with antimicrobial properties. *Food Chemistry*, *194*, 1266–1274.

Iamareerat, B., Singh, M., Sadiq, M. B., & Anal, A. K. (2018). Reinforced cassava starch based edible film incorporated with essential oil and sodium bentonite nanoclay as food packaging material. *Journal of Food Science and Technology*, *55*(5), 1953–1959.

Jorge, C., Fernando, M., Alexandre, E., Caicedo Flaker, C. H., Bittante, A. M. Q. B., & Sobral, P. J. D. A. (2015). Biodegradable films based on gelatin and montmorillonite produced by spreading. *International Journal of Polymer Science*, *2015*, 806791. https://doi.org/10.1155/2015/806791.

Kanmani, P., & Rhim, J. W. (2014). Physicochemical properties of gelatin/silver nanoparticle antimicrobial composite films. *Food Chemistry*, *148*, 162–169.

Khan, M. R., Sadiq, M. B., & Mehmood, Z. (2020). Development of edible gelatin composite films enriched with polyphenol loaded nanoemulsions as chicken meat packaging material. *CyTA-Journal of Food*, *18*(1), 137–146.

Kumar, S., Mitra, A., & Halder, D. (2017). *Centella asiatica* leaf mediated synthesis of silver nanocolloid and its application as filler in gelatin based antimicrobial nanocomposite film. *LWT*, *75*, 293–300.

Kumar, S., Shukla, A., Baul, P. P., Mitra, A., & Halder, D. (2018). Biodegradable hybrid nanocomposites of chitosan/gelatin and silver nanoparticles for active food packaging applications. *Food Packaging and Shelf Life*, *16*, 178–184.

Lee, C., Kim, J. Y., Lee, W. I., Nelson, K. L., Yoon, J., & Sedlak, D. L. (2008). Bactericidal effect of zero-valent iron nanoparticles on *Escherichia coli*. *Environmental Science & Technology*, *42*(13), 4927–4933.

Lin, C. M., Preston, J. F., III, & Wei, C. I. (2000). Antibacterial mechanism of allyl isothiocyanate. *Journal of Food Protection*, *63*(6), 727–734.

Liu, F., Antoniou, J., Li, Y., Ma, J., & Zhong, F. (2015). Effect of sodium acetate and drying temperature on physicochemical and thermomechanical properties of gelatin films. *Food Hydrocolloids*, *45*, 140–149.

Maity, D., & Agrawal, D. C. (2007). Synthesis of iron oxide nanoparticles under oxidizing environment and their stabilization in aqueous and non-aqueous media. *Journal of Magnetism and Magnetic Materials*, *308* (1), 46–55.

Marvizadeh, M. M., Oladzadabbasabadi, N., Nafchi, A. M., & Jokar, M. (2017). Preparation and characterization of bionanocomposite film based on tapioca starch/bovine gelatin/nanorod zinc oxide. *International Journal of Biological Macromolecules*, *99*, 1–7.

Nafchi, A. M., Nassiri, R., Sheibani, S., Ariffin, F., & Karim, A. A. (2013). Preparation and characterization of bionanocomposite films filled with nanorod-rich zinc oxide. *Carbohydrate polymers*, *96*(1), 233-239.

Nassiri, R. (2018). Antimicrobial and barrier properties of bovine gelatin films reinforced by nano TiO2. *Journal of Chemical Health Risks*, *3*(3), 21–28.

Nur Hanani, Z., Beatty, E., Roos, Y., Morris, M., & Kerry, J. (2013). Development and characterization of biodegradable composite films based on gelatin derived from beef, pork and fish sources. *Food*, *2*(1), 1–17.

Paul, S. S. J. P., Saikia, J. P., Samdarshi, S. K., & Konwar, B. K. (2009). Investigation of antioxidant property of iron oxide particles by 1′-1′ diphenylpicryl-hydrazyle (DPPH) method. *Journal of Magnetism and Magnetic Materials*, *321*(21), 3621–3623.

Priya, D. S., Suriyaprabha, R., Yuvakkumar, R., & Rajendran, V. (2014). Chitosan-incorporated different nanocomposite HPMC films for food preservation. *Journal of Nanoparticle Research*, *16*(2), 2248.

Radi, M., Firouzi, E., Akhavan, H., & Amiri, S. (2017). Effect of gelatin-based edible coatings incorporated with Aloe vera and black and green tea extracts on the shelf life of fresh-cut oranges. *Journal of Food Quality*, *2017*, 9764650. https://doi.org/10.1155/2017/9764650.

Rana, D., Mandal, B. M., & Bhattacharyya, S. N. (1993). Miscibility and phase diagrams of poly (phenyl acrylate) and poly (styrene-co-acrylonitrile) blends. *Polymer*, *34*(7), 1454–1459.

Rana, D., Mandal, B. M., & Bhattacharyya, S. N. (1996). Analogue calorimetric studies of blends of poly (vinyl ester) s and polyacrylates. *Macromolecules*, *29*(5), 1579–1583.

Rubentheren, V., Ward, T. A., Chee, C. Y., & Tang, C. K. (2015). Processing and analysis of chitosan nanocomposites reinforced with chitin whiskers and tannic acid as a crosslinker. *Carbohydrate Polymers*, *115*, 379–387.

Sadiq, M. B., Hanpithakpong, W., Tarning, J., & Anal, A. K. (2015). Screening of phytochemicals and in vitro evaluation of antibacterial and antioxidant activities of leaves, pods and bark extracts of *Acacia nilotica* (L.) Del. *Industrial Crops and Products*, *77*, 873–882.

Sahraee, S., Ghanbarzadeh, B., Milani, J. M., & Hamishehkar, H. (2017). Development of gelatin bionanocomposite films containing chitin and ZnO nanoparticles. *Food and Bioprocess Technology*, *10*(8), 1441–1453.

Samsi, M. S., Kamari, A., Din, S. M., & Lazar, G. (2019). Synthesis, characterization and application of gelatin–carboxymethyl cellulose blend films for preservation of cherry tomatoes and grapes. *Journal of Food Science and Technology*, *56*(6), 3099–3108.

Shankar, S., Jaiswal, L., & Rhim, J. W. (2016). Gelatin-based nanocomposite films: Potential use in antimicrobial active packaging. In *Antimicrobial food packaging* (pp. 339–348). San Diego, CA: Academic Press.

Shankar, S., Teng, X., Li, G., & Rhim, J. W. (2015). Preparation, characterization, and antimicrobial activity of gelatin/ZnO nanocomposite films. *Food Hydrocolloids*, *45*, 264–271.

Shankar, S., Wang, L. F., & Rhim, J. W. (2019). Effect of melanin nanoparticles on the mechanical, water vapor barrier, and antioxidant properties of gelatin-based films for food packaging application. *Food Packaging and Shelf Life*, *21*, 100363.

Singh, N., Jenkins, G. J., Asadi, R., & Doak, S. H. (2010). Potential toxicity of superparamagnetic iron oxide nanoparticles (SPION). *Nano Reviews*, *1*(1), 5358.

Tornuk, F., Hancer, M., Sagdic, O., & Yetim, H. (2015). LLDPE based food packaging incorporated with nanoclays grafted with bioactive compounds to extend shelf life of some meat products. *LWT-Food Science and Technology*, *64*(2), 540–546.

Tran, N., Mir, A., Mallik, D., Sinha, A., Nayar, S., & Webster, T. J. (2010). Bactericidal effect of iron oxide nanoparticles on *Staphylococcus aureus*. *International Journal of Nanomedicine*, *5*, 277.

Vanin, F. M., Hirano, M. H., Carvalho, R. A., Moraes, I. C. F., Bittante, A. M. Q. B., & do Amaral Sobral, P. J. (2014). Development of active gelatin-based nanocomposite films produced in an automatic spreader. *Food Research International*, *63*, 16–24.

Voon, H. C., Bhat, R., Easa, A. M., Liong, M. T., & Karim, A. A. (2012). Effect of addition of halloysite nanoclay and SiO 2 nanoparticles on barrier and mechanical properties of bovine gelatin films. *Food and Bioprocess Technology*, *5*(5), 1766–1774.

Zhu, N., Ji, H., Yu, P., Niu, J., Farooq, M. U., Akram, M. W., … & Niu, X. (2018). Surface modification of magnetic iron oxide nanoparticles. *Nanomaterials*, *8*(10), 810.

SUPPORTING INFORMATION

Additional supporting information may be found online in the Supporting Information section at the end of this article.

How to cite this article: Mehmood Z, Sadiq MB, Khan MR. Gelatin nanocomposite films incorporated with magnetic iron oxide nanoparticles for shelf life extension of grapes. *J Food Saf*. 2020;40:e12814. https://doi.org/10.1111/jfs.12814